Available online at www.sciencedirect.com
SCIENCE DIRECT
ELSEVIER
Journal of the European Ceramic Society 26 (2006) 2519–2526
ECERS
www.elsevier.com/locate/jeurceramsoc

Sinter-crystallization in the diopside–albite system Part II. Kinetics of crystallization and sintering

Alexander Karamanov *, Mario Pelino

Department of Chemical Engineering and Materials, University of L'Aquila, Monteluco di Roio 67100, Italy

Received 7 May 2005; received in revised form 28 November 2005; accepted 3 December 2005
Available online 18 January 2006

Abstract

The formation of intragranular pores, induced by diopside crystallization in diopside–albite glasses, was highlighted in a previous study and here confirmed by SEM observation. The sinter-crystallization kinetics of four glass compositions, labelled G1, G2, G3 and G2-Cr, characterized by the formation of *induced crystallisation porosity*, P_{CR}, was investigated. The activation energies of crystallisation, E_C, and sintering, E_S, were evaluated by differential thermal analysis (DTA) and by contact differential dilatometer in non-isothermal conditions, respectively.

The results highlighted that the kinetics of the crystallization process was not influenced by the P_{CR} formation and that the E_C values are in agreement with the corresponding activation energies of viscous flow.

The sintering was evaluated up to 24% linear shrinkage of the samples. In the initial stage of the densification, up to 8% shrinkage, the measured E_S values are comparable for all glasses while, between 9 and 24% shrinkage, E_S increase as a function of the crystallisation ability of each glass. Bulk nucleation occurred in G2-Cr: the rate of phase formation resulted to be higher, the densification was inhibited by the formation of 6 ± 3 wt.% diopside and significant open porosity remained in the sintered glass-ceramic.

Keywords: Sintering; Crystallization; Glass-ceramics; Diopside; Albite

1. Introduction

Glass-ceramics materials have been obtained by sinter-crystallisation technique, using glass powders or frits.[1,2] However, since the densification and the phase formation occur simultaneously, the existing theoretical models, applied to this method, are not able to explain all complex aspects arising during the heat-treatment.[3]

Due to the increasing of the apparent viscosity, the crystallization may reduce or even hinder the sintering, leading to the formation of materials with a residual porosity. At the same time, the formation of crystal phases might avoid the deformation at higher sintering temperature.

The crystallisation lowers the sintering rate and, due to the density variation associated with the phase formation, might also produce an additional porosity. The formation of this *induced crystallisation porosity*, P_{CR}, was highlighted and investigated in the first part of present work.[3] It was demonstrated that the volume variation due to crystallization is partly transformed into shrinkage of the sample and partly into the formation of intragranular spherical pores. The higher is the crystallisation ability of the glass, the lower is the shrinkage and the higher is P_{CR} formation.

In the first part of this study the role played by the formation of the *induced crystallisation porosity* on the crystal growth mechanism was not clarified. In order to highlight this aspect, the crystallisation was investigated by DTA and the obtained activation energies of crystallization were compared with the corresponding activation energies of viscous flow. These results are discussed in the present work, together with the variations of the activation energies of sintering, evaluated by non-isothermal dilatometry. The influence of the crystal phase formation on the densification rate was studied by XRD and SEM techniques.

1.1. Crystallization kinetics

The kinetics of isothermal crystallization in glasses is usually investigated by the KJMA (Kolmogorov, Johnson, Mehl,

* Corresponding author. Tel.: +39 0862 434233; fax: +39 0862 434233.
E-mail address: karama@ing.univaq.it (A. Karamanov).

0955-2219/$ – see front matter © 2005 Elsevier Ltd. All rights reserved.
doi:10.1016/j.jeurceramsoc.2005.12.007

Avrami) equation in the form[1,2,4]:

$$\alpha(\tau) = 1 - \exp(-\text{const}\, I_o U^n \tau^{n+1}) \quad (1)$$

where $\alpha(\tau)$ is the degree of transformation at time τ, I_o the rate of steady-state nucleation, U the rate of crystal growth and n a parameter depending on the crystal growth mechanism and morphology. When no nucleation takes place and the crystals grow on a fixed number of previously formed nuclei, N, Eq. (1) becomes:

$$\alpha(\tau) = 1 - \exp(-\text{const}\, N U^n \tau^n) \quad (2)$$

In the common case of normal growth mechanism, U may be represented by the following relationship[2,4]:

$$U(T) \approx \frac{\text{const}\,\Delta T}{\eta} \quad (3)$$

where ΔT is the degree of supercooling (i.e., the difference between the liquidus, T_l, and the experimental, T_e, temperatures) and η the viscosity. At high temperatures, i.e., close to T_l, U mainly depends on ΔT, while at low temperatures it is a function of the viscosity variation. At high supercooling, the ΔT variation becomes negligible and it may be assumed that the activation energies of crystal growth, E_G, has a value, similar to the corresponding activation energy of the viscous flow, E_η.[2,4] In the glass forming melts E_η decreases with increasing temperature[5,6] but, for a relatively short temperature interval, it may be assumed as constant and evaluated through an Arrhenius equation:

$$\eta(T) = \eta_o \exp\left(\frac{E_\eta}{RT}\right) \quad (4)$$

In the case of non-isothermal crystallization, carried out by DTA or DSC, it is assumed that Eqs. (1) and (2) can be applied in non-isothermal conditions.[7] The non-isothermal kinetics are usually investigated by experiments carried out at different heating rates, ν, and the activation energy of crystallization, E_C, may be evaluated by Chen's equation[8]:

$$\frac{E_C}{RT_\alpha} = \ln\left(\frac{T_\alpha^2}{\nu}\right) \quad (5)$$

where T_α is the temperature, at which α attains equal value at different heating rates. Usually T_α is evaluated at the crystallisation onset temperature, T_o, (corresponding to the beginning of the phase formation) and the peak temperature, T_P, (corresponding to α of 0.63).[4,7] In the last case, Eq. (5) becomes identical to the widely applied Kissinger equation.[9] Using the variation of the glass transition temperature, T_g, with the heating rate, the energy of viscous flow in the glass transition range, E_{Tg}, may also be estimated by Eq. (5).[5,8]

When surface crystallization takes place or when the crystals grow on a fixed number of nuclei, the E_C value corresponds to the activation energy of crystal growth, E_G; when nucleation takes place during heating, E_C has a lower value.[7,10] This is a consequence of the fact that the number of formed nuclei depends on the heating rate: the lower is the rate, the bigger is the number of formed nuclei and the faster will be the phase formation.

1.2. Sintering kinetics

The sintering of glass powders is accompanied by a shrinkage, which depends on the initial porosity, P, of the sample. At 35–40% P the linear shrinkage, $\Delta L/L_o$, corresponding to the formation of a non-porous material, is 13.5–15.5%. The first 10–12.5% are related to neck formation and growth[11,12] and may be expressed by the Frenkel equation[13]:

$$\frac{d(\Delta L/L_o)}{dt} = \frac{3\sigma}{8r\eta(T)} \quad (6)$$

where σ is the surface tension, η the viscosity and r the radius of the particles. Since σ varies little with the temperature, the sintering kinetics depend on the viscosity (i.e., it may be assumed that the activation energy of the sintering, E_S, is equal to E_η). Rewriting Eq. (6) for the case of non-isothermal sintering (i.e., $T = \nu t$) and expressing η by Eq. (4) the following relationship is obtained:

$$\frac{d(\Delta L/L_o)}{dT} = \frac{\text{const}}{\nu} \exp\left(\frac{-E_{sin}}{RT}\right) \quad (7)$$

After integration[8] this relationship gives Chen's equation in the form:

$$\frac{E_{sin}}{RT_X} = \ln\left(\frac{T_X^2}{\nu}\right) \quad (8)$$

where T_X is the temperature at which the sintering process attains a fixed shrinkage value X.

2. Experimental

The theoretical compositions of the studied glasses (labelled G1, G2, G2-Cr and G3) are reported in Table 1. In G2-Cr a 0.3 mol% Cr_2O_3 was added in order to favour bulk crystallization.

The energy of viscous flow in the glass transition range and the activation energies of crystallisation were evaluated by DTA results (Linseiz L81), obtained at 2.5, 5, 7.5, 10 and 20 °C/min using 100–110 mg powder samples (75–125 μm). E_{Tg} was evaluated by T_g variations while the activation energies E_o and E_P—by the variations of T_o and T_P, respectively.

The sintering was studied by 7.5/4.0/4.0 mm^3 "green" samples, prepared by 75–125 μm glass powder fractions, pressed at 100 MPa. After 30 min holding at 270 °C (to eliminate the PVA binder) the samples were heated at 2.5, 5, 10 and 20 °C/min in a differential dilatometer (Netzsch 402 ED). In this instrument,

Table 1
Chemical compositions of the studied glasses (mol%)

	G1	G2	G2-Cr	G3
SiO_2	54	58	58	62
Al_2O_3	2	4	4	6
Cr_2O_3	–	–	0.3	–
CaO	21	17	17	13
MgO	21	17	17	13
Na_2O	2	4	4	6

the dilatometric push rod applies some pressure on the samples, which accelerates the densification and induces some degree of anisotropy.[14,15]

The phase analysis of the samples was made by X-ray diffraction (Philips PW1830 with Cu Kα radiation). The amount of crystalline phase was evaluated by comparing the amorphous and crystalline areas in the XRD spectra.[1] The sintered samples were observed by SEM (Philips XL30CP).

3. Results and discussion

3.1. Crystallisation

Due to the high crystallisation ability of the investigated glasses, the viscosity versus temperature curves could not be experimentally obtained. For this reason the VFT (Vogel-Fulcher-Tammann) equations were calculated by the Lakatos method.[5] It was shown[16] that the hypothetical viscosity versus temperature curves of the investigated compositions are very similar: the calculated T_g temperatures ($10^{13.3}$ dPa s) are in the range 610–625 °C, the Littleton temperatures ($10^{7.6}$ dPa s)—at 820–830 °C and the working points (10^4 dPa s)—at 1140–1170 °C, respectively. These viscosity curves were used to estimate E_η for different temperature ranges and the obtained values are summarised in Table 2.

The DTA curves of the investigated glasses, obtained at 5 °C/min (dashed lines) and 20 °C/min (solid lines), are plotted in Fig. 1. They show similar glass transition temperatures for all glasses, while the crystallisation onset temperature and the peak temperature decrease as a function of the crystallization ability. Compared to G2, T_o and T_P of G2-Cr decrease by 10–15 °C due to the Cr_2O_3 addition. The bulk nucleation in G2-Cr was confirmed by other DTA experiments where powders of each glass were held for 1 h at 750 °C (for nucleation) and then heated up to 1100 °C: in G1, G2 and G3 no variations were observed, while in G2-Cr T_o and T_P decreased by another 10–20 °C.

The variations of T_g, T_o and T_P as function of the heating rate are presented in Figs. 2–4, respectively, while Table 3 summarised the E_{Tg}, E_o and E_P results, obtained by Chen's relationship. All E_{Tg} values are in the narrow range between 580–620 kJ/mol, thus confirming the similarity of the viscosities, while E_o and E_P varied from 360 to 510 kJ/mol and from 340 to 485 kJ/mol, respectively.

Varying the crystallisation ability among G1, G2 and G3, T_o and T_P decrease, while E_C increase. The E_C variations may be explained considering that during a surface crystallization process, E_C has a value similar to the activation energy of viscous flow. In fact, as shown in Tables 2 and 3, the obtained E_o and E_P are in agreement with the hypothetical temperature variations of the E_η.

Table 2
Variation of the activation energy of viscous flow vs. temperature

	G1 (KJ/mol)	G2 (KJ/mol)	G3 (KJ/mol)
600–700	595	576	556
700–800	472	457	442
800–900	397	385	373
900–1000	348	337	327
1000–1100	313	303	294

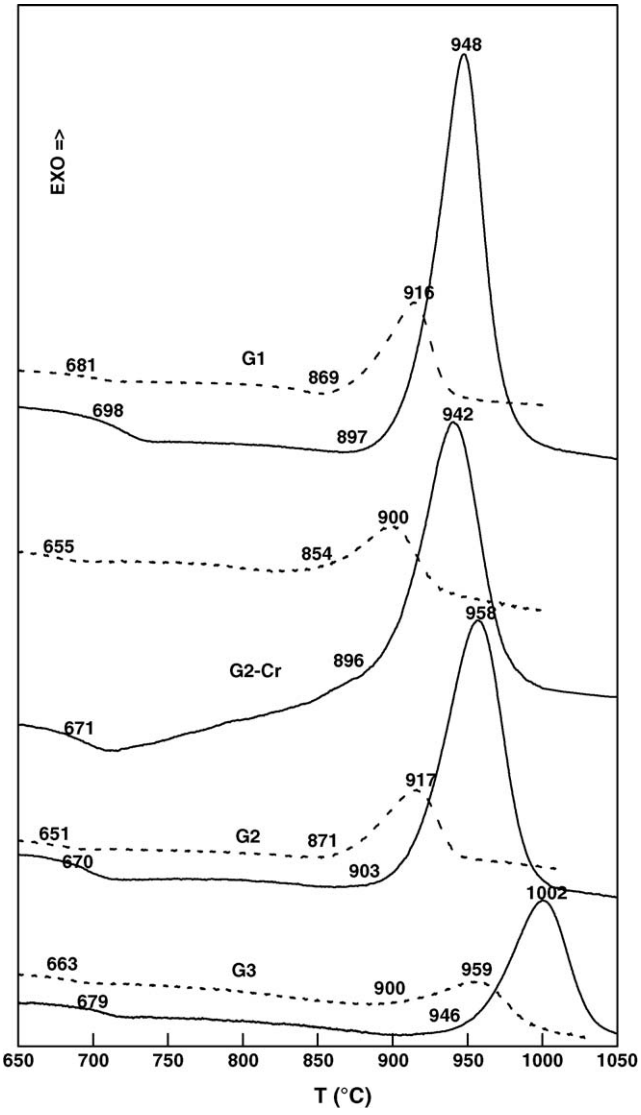

Fig. 1. DTA traces of the investigated glasses at 5 and 20 °C/min.

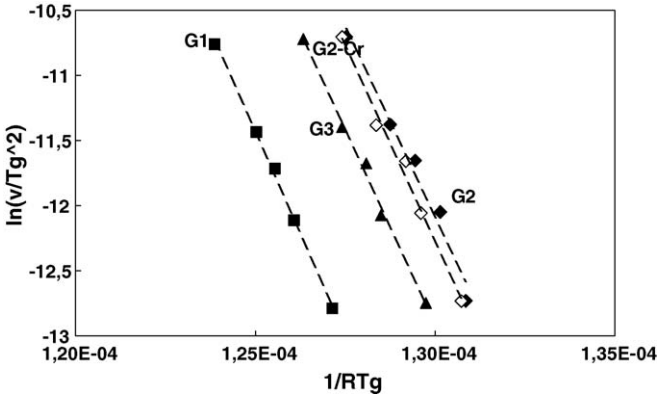

Fig. 2. Variations of T_g vs. temperature, obtained by Chen's equation.

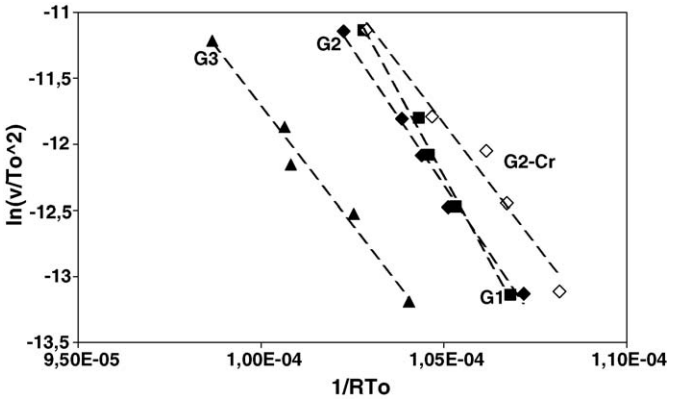

Fig. 3. Variations of T_o vs. temperature, obtained by Chen's equation.

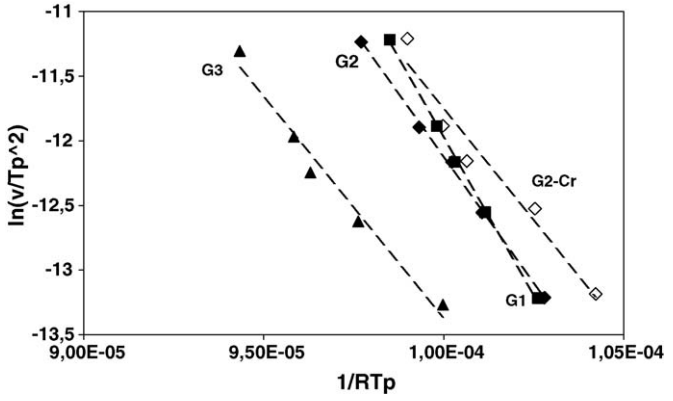

Fig. 4. Variations of T_P vs. temperature, obtained by Chen's equation.

In G2-Cr, due to the addition of Cr_2O_3, the crystallisation temperatures and the crystallisation activation energies decrease with respect to G2. The bulk crystallisation increases the rate of phase formation and the DTA peaks are observed at lower temperature; the E_C values become lower than the activation energy of crystal growth E_G.[7,10]

The surface crystallization in G1, G2 and G3 and the occurrence of bulk crystallization in G2-Cr were confirmed by BSE-SEM microscopy, using polished specimens etched for 3 s with 2 wt.% HF.

Fig. 5 is an image of G1 sample after 1 h at 800 °C, showing a sintered body with a residual intergranular porosity and surface crystallization between the grains. Fig. 6a shows G2-Cr sample after 1 h at 800 °C: the crystalline formation is evident between the grains as well as in the bulk of the particles. Fig. 6b is a

Table 3
Activation energies of viscous flow in the glass-transition range, E_{Tg}, and crystallization, E_o and E_P

	G1	G2	G2-Cr	G3
E_g (KJ/mol)	621	582	598	595
Temperature range (°C)	673–698	646–670	647–671	654–679
E_o (KJ/mol)	507	409	360	357
Temperature range (°C)	853–897	849–903	839–896	883–946
E_P (KJ/mol)	485	387	342	341
Temperature range (°C)	899–948	897–958	881–942	930–1002

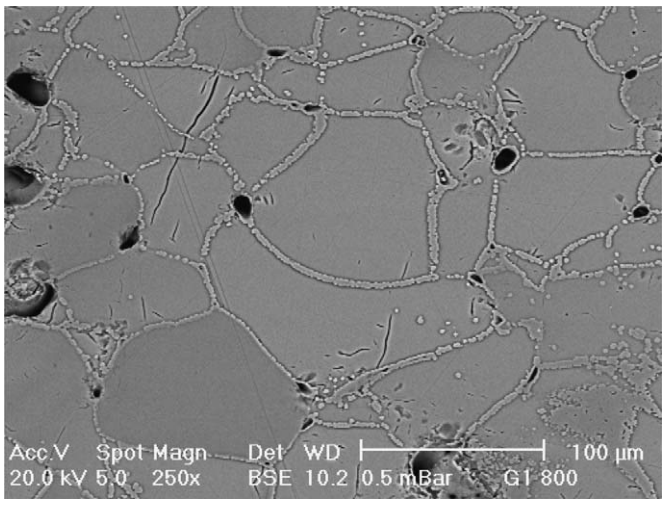

Fig. 5. BSE-SEM images of polished G1 sample, sinter-crystallised at 800 °C.

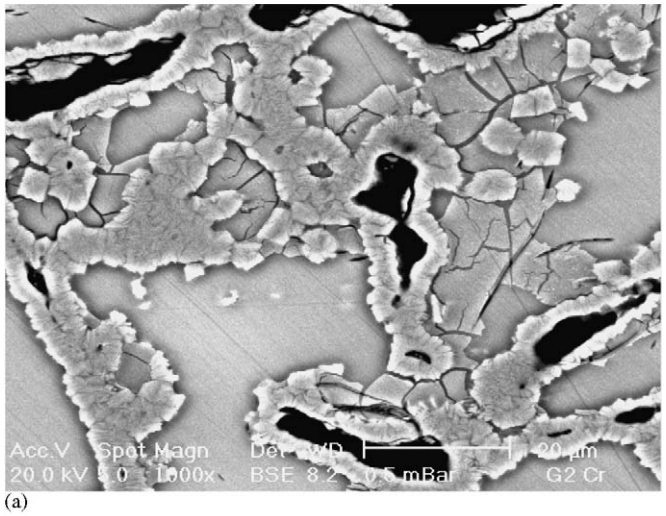

(a)

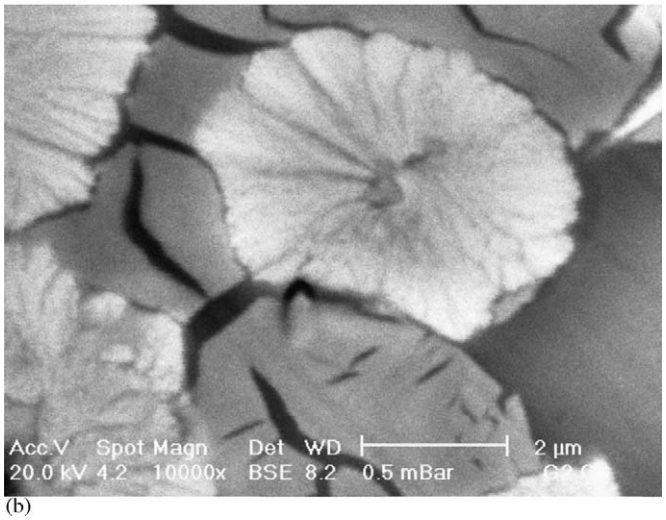

(b)

Fig. 6. BSE-SEM images of polished G2-Cr sample, sinter-crystallised at 800 °C.

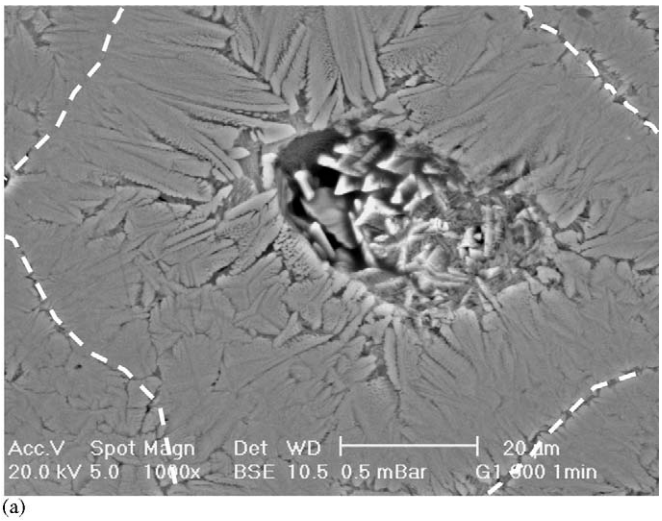

(a)

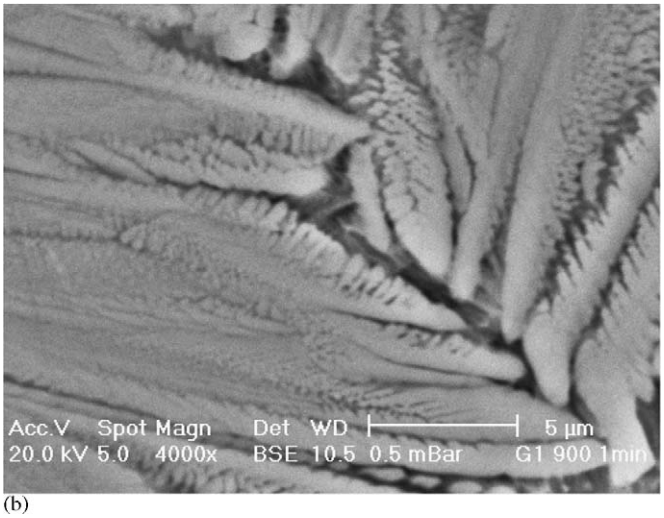

(b)

Fig. 7. BSE-SEM images of polished G1 sample, sinter-crystallised at 900 °C.

10,000 magnification of a diopside spherulite in the bulk. Fig. 7a is an image of Fig. 5 sample, heat-treated at 900 °C and shows a *induced crystallization pore* in the centre of the particle. The grain boundaries are marked by the dashed white line. Fig. 7b is a magnification of 7a with colonnar dendritic crystals growth from the surface toward the centre.

The total percentages of diopside formed in G1, G2 and G3 glass-ceramics were evaluated as 59 ± 1%, 49 ± 1% and 30 ± 1 wt.%, respectively.[3] It was also clarified, that the formation of the *induced crystallization porosity* (about 8, 6 and 1 vol% in G1, G2 and G3, respectively) starts after the crystallization of about 12 wt.% diopside in G1, 16% in G2 and 23% in G3. A P_{CR} value of about 5%, was also evaluated in G2-Cr glass-ceramic.

From these results it was inferred that no *induced crystallization porosity* is formed during the beginning of the crystallization process (evaluated by T_o), whereas P_{CR} formation takes place in G1, G2 and G2-Cr during the diopside formation indicated by T_P. For G3 the P_{CR} formation is negligible. At the same time, E_P and E_o have comparable values for all compositions, with a difference of about 20 KJ/mol due to the 40–50 °C temperature

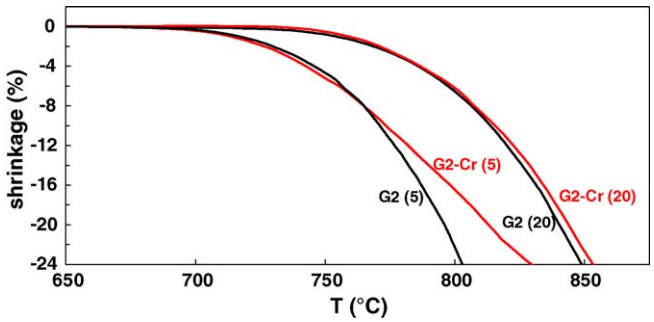

Fig. 8. Dilatometric traces of G2 and G2-Cr at 5 and 20 °C/min.

difference between the T_P and T_o ranges. It was concluded that the rate of the phase formation is not influenced by the formation of the *induced crystallization porosity*.

3.2. Sintering

The contact dilatometer, employed in this study, applies some pressure on the sample during the densification. Therefore, the linear shrinkage was measured up to 24% (for the initial length of 7.5 mm size). In the other two directions, the $\Delta L/L_o$ was measured as 4.0 ± 0.5% by a micrometer. Considering an initial porosity of 35 vol%,[3] it was evaluated that about 7 vol% residual porosity remained in the samples at 24% linear shrinkage.

The four compositions show similar dilatometric traces: the sintering onset temperatures are near to the corresponding T_g temperatures, a 1% shrinkage is obtained at 700–750 °C and a 24%—at 770–880 °C. For G1, G2 and G3, the sintering rate increases continuously with the temperature at all heating rates. G2-Cr shows similar behaviour at 10 and 20 °C/min, while at 2.5 and 5 °C/min the sintering rate starts to decreases after a $\Delta L/L_o$ of about 12%. This behaviour is shown in Fig. 8, where the G2 and G2-Cr traces at 5 and 20 °C/min are compared.

The variations of the sintering activation energy as a function of the shrinkage are plotted in Fig. 9. At $\Delta L/L_o$ up to 8% the measured E_S are comparable for all glasses, but, due to the external force applied by dilatometer push-rod, the obtained values of E_η are 200–250 kJ/mol lower than the expected ones. A similar

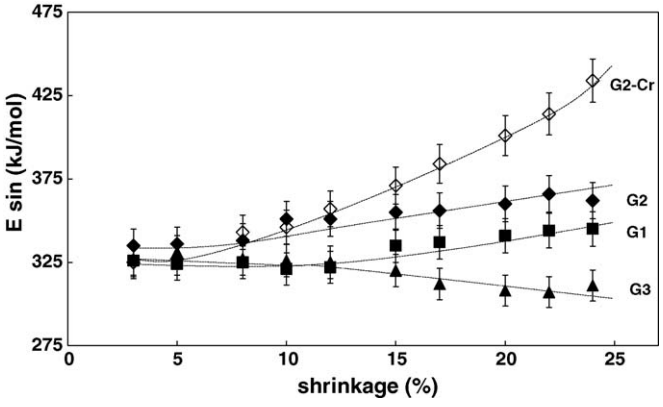

Fig. 9. Variations of the activation energy of sintering as function of the shrinkage.

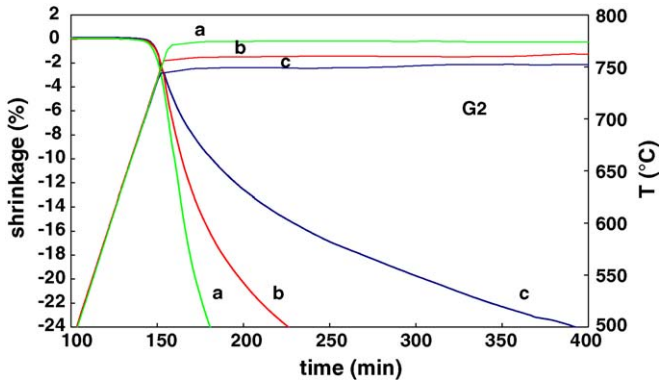

Fig. 10. Isothermal dilatometric plots of G2 at 750, 760 and 770 °C.

difference was also obtained in a previous study carried out on a soda-lime-silica glass.[17]

Between 10 and 24% linear shrinkage, the sintering activation energy varies as a function of the crystallisation trend. E_S decreases in G3, increases in G1, G2 and, especially, in G2-Cr where E_S becomes higher than E_C at $\Delta L/L_o$ of 24%. This behaviour may be explained, assuming that the nucleation and/or the beginning of the phase formation significantly increases the apparent viscosity, η_a,[3,18] thus decreasing the sintering rate and increasing E_S.

In order to highlight this phenomenon, G2 and G2-Cr samples were heat-treated at 5 °C/min and held for 5 h at 750, 760 and 770 °C. The results are plotted in Figs. 10 and 11 and show that in both compositions the sintering starts at about 700 °C and have a similar behaviour up to 8% shrinkage. Then, the sintering rate in G2-Cr starts to decreases becoming zero after about 1, 2 and 4 h holding at 770, 760 and 750 °C, respectively.

The viscosity variations, in the investigated 650–800 °C range, were estimated by the Lakatos method,[5] assuming a T_g temperature of 650 °C. In this manner, for the initial shear viscosity, η, at 700, 750, 760 and 770 °C the values of $10^{11.5}$, $10^{10.1}$, $10^{9.8}$ and $10^{9.5}$ dPa s were obtained, respectively. It can be calculated that η decreases by a factor of ≈2 every 10 °C which means that, according to Eq. (6), the sintering time at 750 °C must be about two- and four-times longer than the sintering times at 760 and 770 °C, respectively.

The experimental results are quite different. Fig. 10 shows that in G2 a 24% $\Delta L/L_o$ is reached after 225–230 min holding time at 750 °C, 55–60 min at 760 °C and 10–15 min at 770 °C, respectively. Fig. 11 shows that in G2-Cr the sintering stops at about 16, 20 and 22.5% linear shrinkage (corresponding to a residual porosity of about 16, 12 and 9 vol%) after holding at 750, 760 and 770 °C, respectively.

The sintering behaviour of G2 and G2-Cr was also investigated by SEM, using samples heat-treated at 5 °C/min, held for 1, 5 and 120 min at 800 °C and cooled at 10 °C/min. The images of the G2 and G2-Cr fractured samples are shown in Figs. 12 and 13, respectively. After 1 min holding, the two samples show a similar neck formation stage; after 5 min—the sin-

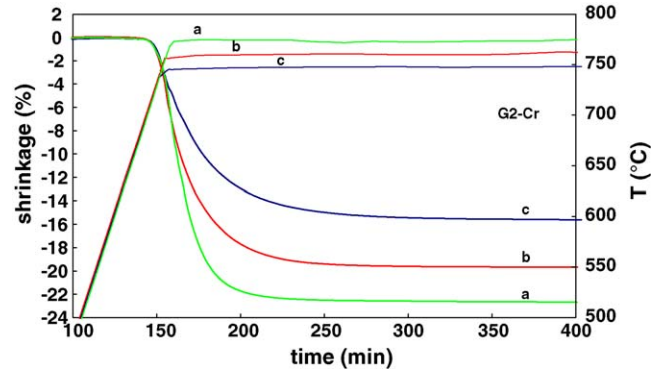

Fig. 11. Isothermal dilatometric plots of G2-Cr at 750, 760 and 770 °C.

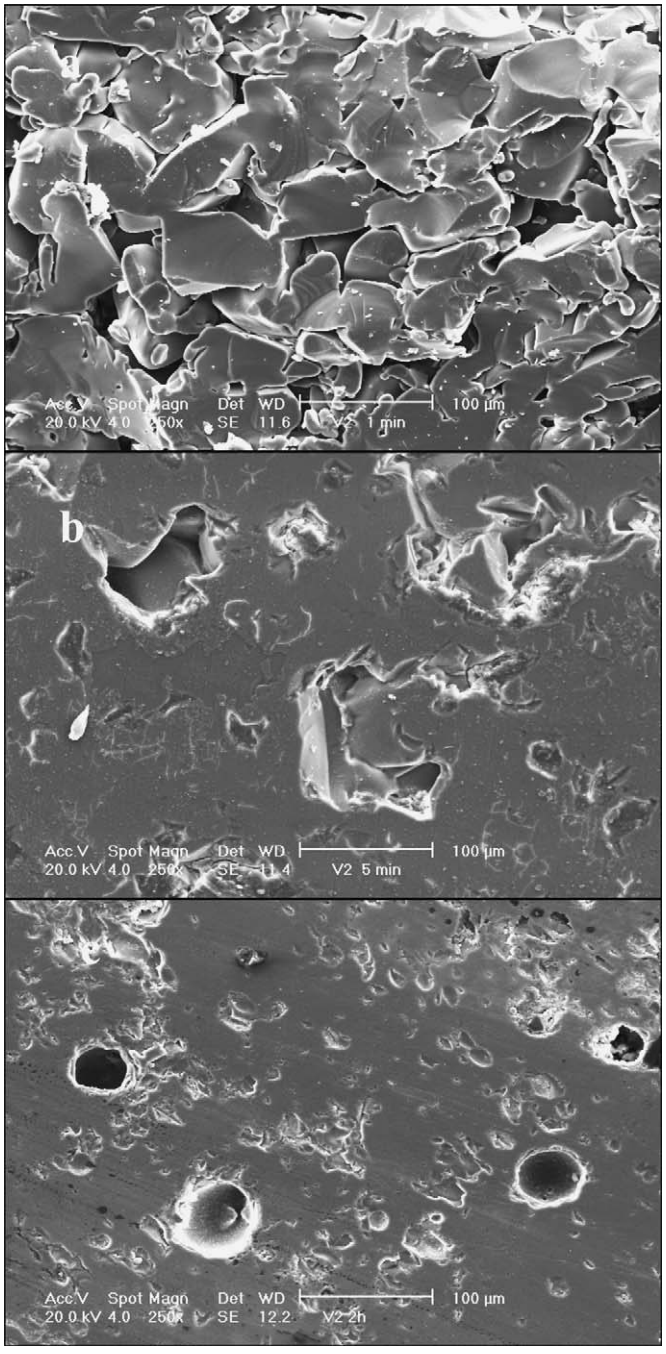

Fig. 12. SEM images of fractured G2 samples, sintered for 1 min (a), 5 min (b) and 120 min (c) at 800 °C.

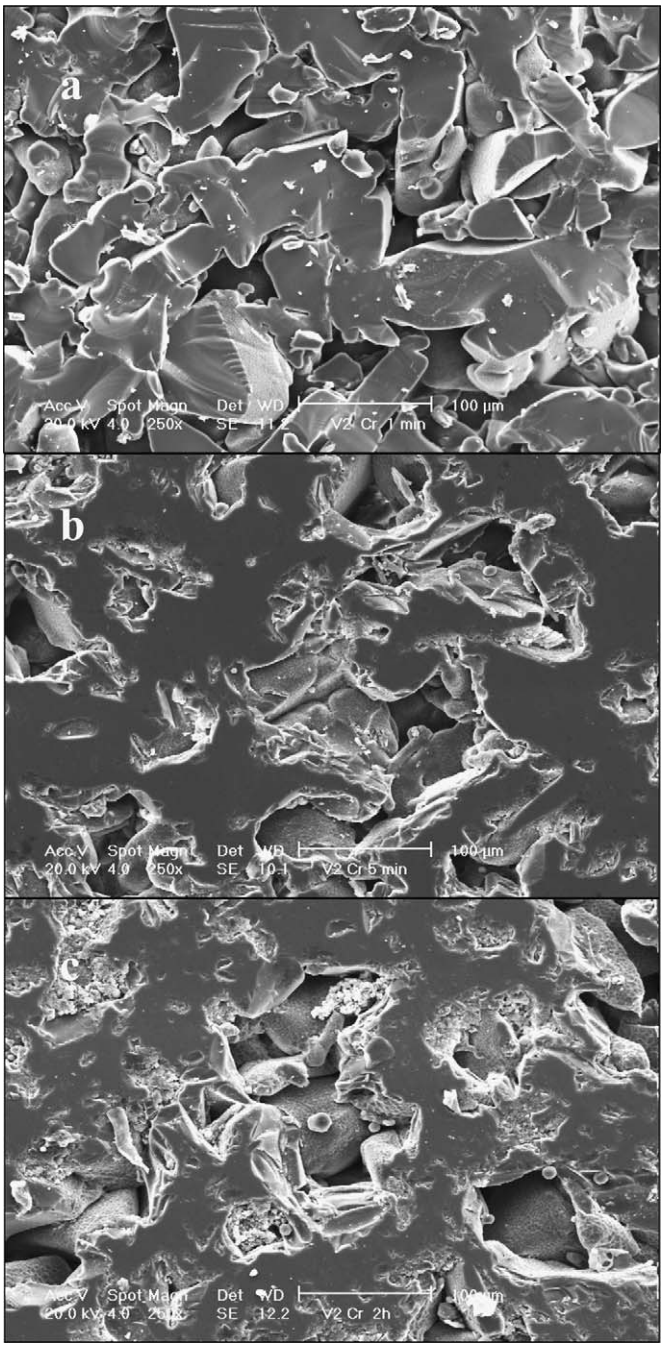

Fig. 13. SEM images of fractured G2-Cr samples, sintered for 1 min (a), 5 min (b) and 120 min (c) at 800 °C.

tering improves in both samples but the degree of densification is higher in G2; after 120 min—the densification is completed in G2 (only some residual closed porosity is observed), while G2-Cr shows an open porosity similar to one at 5 min sintering.

The amount of crystal phase formed in G2-Cr was investigated by XRD. Fig. 14 shows the spectra of the parent glass, samples sintered for 1 and 5 h at 760 °C and the final glass-ceramic (1 h at 900 °C). After 1 h at 760 °C, the spectrum is similar to the parent glass; after 5 h the amount of formed diopside was evaluated as $6 \pm 3\%$. It was concluded that the formation of a low amount of crystal phase (10 ± 5 wt.%)[3,19,20]

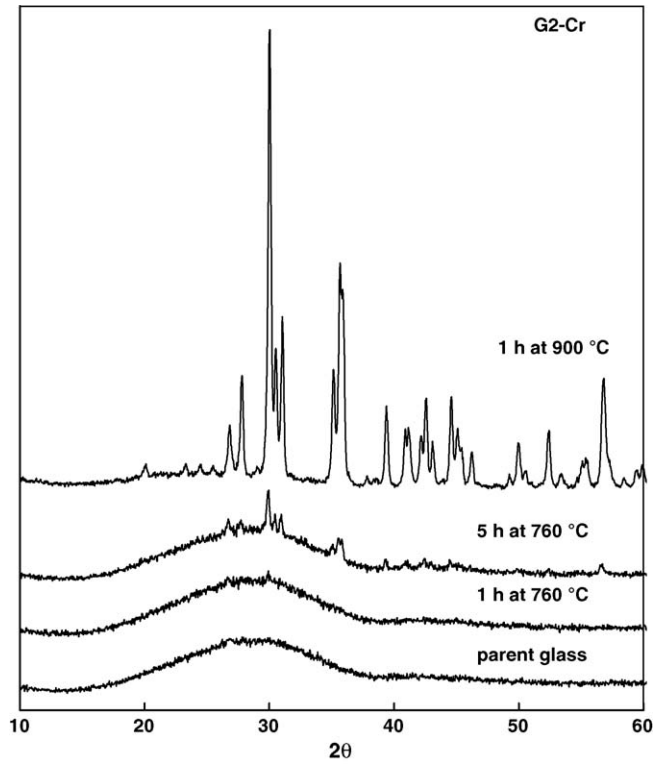

Fig. 14. Spectra of G2-Cr samples, sintered at 760 °C, parent glass and final glass-ceramic.

increases the apparent viscosity by more than 100 times (i.e., from $\approx 10^{9-10}$ to $\approx 10^{11-12}$ dPa s), leading to a system of "rigid" particles. The subsequent volume variation, due to the diopside crystallization (up to ≈60% in G1, ≈55% in G2-Cr and ≈50% in G2), does not produce additional shrinkage but is transformed into the formation of a round-shaped intragranular porosity.

4. Conclusions

The investigated diopside–albite glass compositions are characterized by similar T_g temperatures and by comparable activation energies of viscous flow, E_η. The glasses have different crystallisation behaviour leading to various percentage of *induced crystallization porosity*, P_{CR}.[3] The formation of this intragranular porosity has not influence on the crystallization kinetics so that the activation energies of crystallization are always in agreement with the corresponding E_η.

In the initial stage of the densification the activation energies of sintering, E_S, are comparable for all glasses; then E_S increases as a function of the crystallisation ability. In the case of bulk nucleation, the densification stops after the formation of $6 \pm 3\%$ diopside, leading to significant residual open porosity in the glass-ceramic.

References

1. Strnad, Z., *Glass-Ceramic Materials*. Elsevier, Amsterdam, 1986.
2. Hőland, W. and Beall, G., *Glass-Ceramics Technology*. The American Ceramics Society, Westerville, 2002.

3. Karamanov, A. and Pelino, M., Sinter-Crystallization in the system diopside–albite. Part I. Formation of induced crystallisation porosity, J. Eur. Ceram. Soc., in press.
4. Gutzow, I. and Shmelzer, J., *The Vitreous State—Structure, Thermodynamics, Rheology and Crystallisation*. Springer Verlag, Berlin, New York, 1995.
5. Scholze, H., *Glass Nature, Structure and Properties*. Springer-Verlag, Berlin, 1990.
6. Hlavac, J., *The Technology of Glass and Ceramics: An Introduction*. Elsevier, Amsterdam, 1983.
7. Ray, C. S. and Day, D. E., Nucleation and crystallization in glasses as determined by DTA, ceramic transactions. In nucleation and crystallization in liquids and glasses. *Am. Ceram. Soc.*, 1992, **30**, 207–224.
8. Chen, H., A method for evaluating viscosities of metallic glasses from the rates of thermal transformations. *J. Non-Crystal. Solids*, 1978, **27**, 257–263.
9. Kissinger, H., Reaction kinetics in differential thermal analysis. *Anal. Chem.*, 1957, **29**, 1702–1706.
10. Matusita, K. and Sakka, S., Kinetic study on crystallization of glass by differential thermal analysis—criterion on application of Kissinger plot. *J. Non-Crystal. Solids*, 1980, **38**, 741–745.
11. Zanotto, E. and Prado, M., Isothermal sintering with concurrent crystallisation of monodispersed and polydispersed glass particles. Part 1. *Phys. Chem. Glasses 42*, 2001, **3**, 191–198.
12. Olevsky, E., Theory of sintering: from discrete to continuum. *Mater. Sci. Eng.*, 1998, **R23**, 41–100.
13. Frenkel, J., Viscous flow of crystalline bodies under the action of surface tension. *J. Phys. USSR*, 1945, **9**(5), 385–391.
14. Paganelli, M., Using the optical dilatometer to determine sintering behaviour. *Am. Ceram. Soc. Bull.*, 2002, **81**(11), 25–30.
15. Rahaman, M. N. and De Jonghe, L. C., Sintering of spherical glass particles under a uniaxial stress. *J. Am. Ceram. Soc.*, 1990, **71**(3), 707–712.
16. Karamanov, A., Arrizza, L., Matecovetc, I. and Pelino, M., Properties of sintering glass-ceramics belonging to the system diopside–albite. *Ceram. Int.*, 2004, **30**, 2129–2135.
17. Karamanov, A., Aloisi, M. and Pelino, M., Sintering behaviour of a glass obtained from MSWI ash. *J. Eur. Ceram. Soc.*, 2005, **25**, 1531–1540.
18. Gutzow, I., Paskova, R., Karamanov, A. and Schmelzer, J., The kinetics of surface induced sinter-crystallization and the formation of glass-ceramic materials. *J. Mater. Sci.*, 1998, **33**(21), 5265–5273.
19. Karamanov, A., Pelino, M. and Hreglich, A., Sintered glass-ceramics from MSW-incinerator fly ashes. Part I. The influence of the heating rate on the sinter-crystallisation. *J. Eur. Ceram. Soc.*, 2003, **23**, 827–832.
20. Aloisi, M., Karamanov, A. and Pelino, M., The sintering behaviour of MSWI ash glass. *J. Non-Crystal. Solids*, 2004, **345–346**, 192–196.